International Journal of Multidisciplinary Research and Development
Online ISSN: 2349-4182, Print ISSN: 2349-5979; Impact Factor: RJIF 5.72
Received: 03-05-2019; Accepted: 06-06-2019
www.allsubjectjournal.com
Volume 6; Issue 8; August 2019; Page No. 07-13

Removal of heavy metals from industrial wastes of Mobarakeh Isfahan steel with tomato pulp

Sifatullah Shakir[1*], Allah Nazar Atif[2], Sayed Attaul Haq Banuree[3]
[1] Department of Chemistry, Faculty of Sciences, Nangarhar University, Afghanistan
[2] Department of Biology, Faculty of Sciences, Nangarhar University, Afghanistan
[3] Department of Pre-Clinic, Faculty of Veterinary Science, Nangarhar University, Afghanistan

Abstract
The demand for clean water is increasing due to population growth. One of the ways to solve the problem of water scarcity is to treat contaminated water through the removal of pollutants. The use of adsorbents to remove pollutants is one of the promising methods. Tomato pomace is a plant waste, and in this study, its adsorption potential for selected pollutants in water was studied. We report the performance of tomato peel before and after correction with ethylene diamine (EDA) on the adsorption of copper, lead, and cadmium in aqueous solution. The content of the adsorbed substance was 5.27 $mg.g^{-1}$, 2.12 $mg.g^{-1}$ and 2.16 $mg.g^{-1}$ 2.16, respectively, for Cu, Cd and Pb with modified adsorbent, respectively. For unbleached adsorbent, the amounts of $mg.g^{-1}$ were 3.29 $mg.g^{-1}$ 4.57 and 1.05 $mg.g^{-1}$ were reported. The pH for maximum absorption was between pH 4 and pH 6. In a separate study, it was determined that g0.1 was washed out of dried tomato pellets, 20 mg of solvent organic carbon (DOC), using ml of distilled disintegrated distilled water. The solution was green. The leach process causes secondary contamination. Reducing tomato pomace with EDA reduced the content of the DOC by half (50%), and removed the green color. Kinetic studies showed that the absorbent could absorb 95% of the metal in less than 10 minutes (in standard synthetic solution). Then, the adsorbed metals were removed from HNO3 using M0.5 solution, indicating that the adsorbent can be regenerated. In addition, this study showed that the reform improved the absorbent thermal stability so that, even when the temperature increased to 1000˚C, more than 80% of the modified adsorbent (as compared to 50% of the unpolished tomato pumice) did not break down, indicating that These modifications have had a significant impact on the thermal stability of tomato scum.

Keywords: organic carbon, ethylenediamine, metal absorption, modified adsorbent, tomato pulp, sewage

1. Introduction
One of the most important issues in the world today is environmental pollution to toxic and dangerous metals [1-5].
The extraction of metals from mines and the widespread use of heavy metals in the industry have led to an increase in concentrations of these metals in water, sewage, air and soil than in the underlying ones.
The mechanism of the heavy metals toxicity is due to the intense cations of these metals to sulfur and thus disrupts the activity of vital enzymes in living organisms [6-7].
Therefore, the removal of heavy metals from the aquatic environment is an important issue in public health, which is important in two respects:
(A) Separation of toxic heavy metals from industrial effluents, drainage, mines and neutralizing their toxic effects
(B) Recovery and recycling of metals, which is essential if gradually decreasing mineral resources.
Heavy metals in the wastewater of many industries such as the extraction industry of zinc and other heavy metals from ore, petrochemical industry, petroleum refining industry, paper industry, pharmaceutical industry, coloring industry, plastic products industries, etc., and if they go to Sewage treatment systems affect microorganisms and kinetics of sewage treatment reactions due to their toxicity properties, which reduces the efficiency of the system.
This results in the concentration of these compounds in the waste water from the outlet of the refineries not meeting the standard set by the domestic and international authorities. On the other hand, the migration of these heavy elements and compounds into the environment will have irreparable effects on the environment and humans. In view of the above, the purification of these compounds and their removal in accordance with domestic and international standards is of great importance. Heavy metals are essentially a group of metal elements with a specific gravity greater than 6 g / cm2 and a specific gravity of more than 50 [7].
Some of them are considered as essential elements and their presence in the human food chain and other creatures is needed, which is why they are called essential elements. The presence of these elements at excess concentrations has created many adverse effects for humans and for other organisms, while also contributing to environmental pollution and risks. Heavy metals include mercury, arsenic, cadmium, nickel, copper, lead, chromium, zinc, vanadium, etc., which have different welding points [4].
Among the environmental pollutants associated with heavy metals are:
Heavy metal extraction, metal industry, casting, plating, painting, batteries, tannery, textile, paper making and other similar industries that are responsible for the disposal and release of elements such as cadmium, mercury, nickel, lead, zinc, chromium, copper and silver in The environment causes contamination [8-11].
The presence of heavy metals in industrial effluents and environmental problems caused by their non-standard

disposal will require the treatment of such wastewater before discharging into the environment or entering the sewage collection network. Surface water and underground water resources, which are somewhat contaminated with heavy metals, need to be purified. So far, several different methods have been implemented to remove heavy metals from the sewage industry, each with practical and economic advantages and disadvantages [12-16].

In Iran, the effort to control the electrolytic wastewater containing heavy metals is mainly due to the precipitation of heavy metals in the form of sedimentation and distillation of sludge recovered from these metals, so it is predictable that, given the large number of units Plumbing in the country every year, relatively large quantities of these metals, along with wastewater or sludge, are discharged into the environment.

In recent years, bioavailability studies have been intensified to meet this need. Bio-absorbent, physiochemical absorption of heavy metals, reagents (fungi, bacteria, algae) and organic matter (rice bran, pepper and fruit pulp, etc.). Biodegradability can be improved by using physical and chemical pretreatment methods.

2. Materials and Methods

2.1 Chemicals and Reagents

All of the solutions were prepared with double water and the reagents were of analytical grade. Standard metal solutions were prepared in M 0.1 sodium acetate solution to maintain ionic strength. Standard reference solutions for analyzing ICP-OES were prepared from Associated Chemical Supplies Ltd Fluka Analytical Inc. (Buchs, Switzerland). Thionyl chloride and ethylenediamine were prepared from Riedel-de Haën ® (Seelze, Germany) while Sodium acetate, hydrochloric acid and ammonia were supplied from Rochelle Chemicals Ltd (Johannesburg, South Africa).

2.2 Equipment

The metal content of the solution was determined by a spectrophotometric atomic coupling plasma (ICP-OES, OPTIMA 5300DV model) (Shelton, CT, USA). Factor bands affixed to the adsorbent were determined using the infrared Fourier transform (FT-IR) spectrometer (Perkin Elmer 100 made in Waltham, MA, USA). Thermal stability of modified and uncorrected adsorbents was performed by differential scanning calorimetry analysis / Perkin Elmer, DSC-TGA, and SDT Q600 model made by Newcastle DE, USA. This analysis was performed to determine the effect of temperature on bio-degradation (Pielichowski and Pielichowski, 2007). The TGA method provides information based on weight variations as a function of temperature that allows the determination of the decomposition temperature, moisture content, and the level of organic and inorganic compounds in the material. The absorbent was also measured with C NMR solid state, which has opposite polarity / magic rotation angle (CP / MAS). The device used was a Bruker 60013 C NMR spectrometer (Hanau, Germany) operating at a frequency of 10 MHz. The opposite polarity (CP) was adjusted by glycine at 10 kHz and the rotational speed was set at 10,000 Hz. The call time for CP was set to 1 ms and the delay time was 5 s. A comparison of the percentage of nitrogen in both modified and unformed tomato pulp with elemental analysis was performed in an elemental analyzer LECO 932 CHNS (GmbH, Mönchengladbach, Germany). This work was done to determine the relative percentages of carbon, hydrogen and nitrogen in the samples. The results will confirm that i-acetylene-2-diamine is chemically bonded to adsorbent to fix the adsorbent level [9].

2.3 Trial process

2.3.1 Correction of tomato pomace

The g10 from a bioactive material previously activated at 80 ˚C for 12 h was converted into 200 ml of N and N-dimethylformamide (DMF) in suspension, followed by 35 ml of thionyl chloride (SOCl 2) at 80 ˚C under conditions Mechanical stirring was added as a dropper. After completing the addition of this substance, the contradiction continued at the same temperature for 4 h. Chopped tomato pomace was washed several times with an equal amount of dilute ammonium hydroxide solution until the pH of the supernatant is neutralized. The solid portion was then separated by filtration and dried under vacuum conditions at room temperature (Tashiro and Shimura, 1982).

5 grams of neutralized chlorinated tomato pellets were reacted with 25 ml of ethylene 1 and 2-diamine during the reciprocal flow, while it was mechanically inhaled for h3. The solution was then strained with porous glass filter and the solids were dried at room temperature for 24 h for drying. The modified and dried tomato pulp was used for absorption experiments.

2.3.2 Batch Absorption Tests

Absorption studies were carried out using a torn bottle with an SSL2 (Harrogate, UK) laboratory mechanical shuttle. The solution pH of the model contains a specific concentration of metal ions at pH values of between pH 3 and pH 7. A clear weight (g 0.04) of the gravity of each mixture was added and released to provide sufficient time to achieve absorbance equilibrium. The resulting mixture was filtered with Watten Paper No. 42 (No. 42) and liquid metal ions were straightened by ICP-OES.

2.3.3 pH Optimization in Tomato Pomace, Modified and Uncorrected

Tomato pomace (s) were weighed in the approximate amount of 0.04 g each and were poured into bottles of 100 ml polyethylene torsion. Subsequently, 10 ml of a metal solution (mg l-150) prepared in a suitable buffer solution (Sodium Estate M0.1 / acetic acid) with a pH adjusted between 2 and 7 was added. The mixtures were brought to equilibrium for h1, after which the metal was dissolved by ICP-OES.

2.3.4 Optimization of absorption time

Equivalent to 10 ml of solution solutions (mg-150) were distributed in 100 ml polyethylene bottles containing 0.04 g of each of the adsorbents, as modified and unpolished tomato pomace. The initial pH of the model solution was adjusted to the optimal value for each of the studied metals. Copper at pH was adjusted to 5.5 for both modified and uncorrected adsorbents. Cadmium was adjusted at pH values of 6.2 and 5, respectively, for modified and unpolished adsorbants. While lead was adjusted to pH 4.5-5 for the modified and unpolished adsorbent. The corresponding mixtures reached the equilibrium and then left the shaker at different time intervals. The organic matter was filtered and filtered by suction and the concentration of metallic ions in the stratified liquid was determined by ICP-OES.

2.3.5 Determination of the extracted organic soluble organic carbon (DOC) in water

The DOC was determined by the process that Oweczkin *et al*. (1996) proposed using ICP-OES to determine the organic carbon contained in the soil samples. Standard solution of carbon from sucrose was prepared in the range of 10-100 mg l-1. The specimen was prepared by adding a certain weight of the absorber (0.1 g) to a 250 milliliter barrel containing 100 ml of a double tap water. The mixture was placed on a magnetic stirrer and stirred for 1 h to dissolve the organic compounds. The solid was filtered and strained and the organic carbon content was determined by ICP-OES.

2.3.6 Capacity of absorbed tomato modified and not modified

Absorption capacity was determined by changing the initial concentration of metal ions in 10-ml strains of model solutions containing approximately 0.04 g of each biomaterial. The pH was adjusted to the desired amount of each metal and the mixture was stirred for 1 h on a mechanical shaker. The preparation, the smooth mixture, and the content of liquid metal dissolved by ICP-OES were determined.

2.3.7 Analysis of Mobarakeh Steel Samples in Isfahan

Mobarakeh industrial water samples were collected and individual concentrations of lead, copper and cadmium ions were entered into each of the samples (ml50). The mixtures were extracted on a solid phase extraction column (SPE) containing 0.4 g of adsorbent and the remaining metal was removed with 0.5 M nitric acid.

3. Results and Discussion

3.1 FTIR Results

The refined and unsweetened adsorbents were measured by FTIR and the spectra obtained are presented in Fig. 1. shows the microscopic image of different absorbents. As shown in the figure, in the unmodified mode, the particle size is larger and the cavities in the modified state are larger. But the cavities in the modified state are thinner and more dispersed, which can help to absorb contaminants of water.

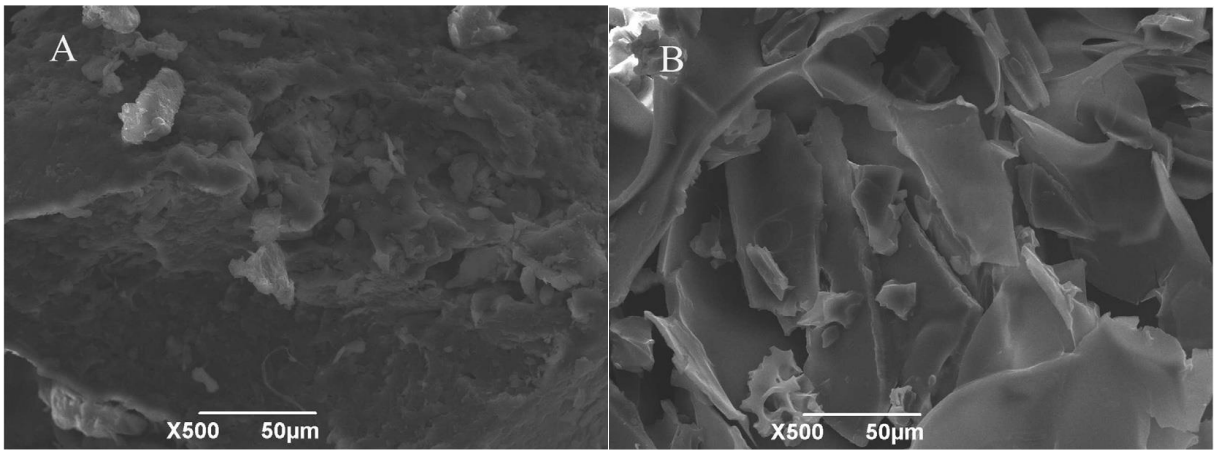

Fig 1: (A) Modified **(B)** Unmodified

The FTIR spectrum is a testament to the presence of many functional groups that allow metal to be absorbed. Fig. 2 A shows a strong band of 3404.31 cm-1 relative to both -OH and -NH groups (Stuart, 1996); however, it shows Bonddupic, thus indicating that it is probably more due to Gro-NH (Stuart, 1996). The band at 12928.72 cm was related to the vibrations of C-H, while the band at 1612.13 cm-1 corresponded to -OH or N = C vibrations. The band in cm-11728.91 can be derived from the C = O carbonyl functional group. A band of 1317.11 cm-1 can be obtained from an amide or sulfamide group. The bond in 11,227.27 cm is attributed to organic sulfate (Khazaei *et al*., 2007). This indicates the presence of sulfur in the adsorbent. This displacement of the band in cm-1 is 1626.65-1612.13 (after correction) and the appearance of a band in cm-11531.12 (shown in Fig. 4-1 B) due to the change in the angle of NH (amine group), which indicates the stabilization of ethylene-Dyamine is on tomato pomace. The band at 1317.11 cm-1 also changed to 1331.45 cm -1, which was mentioned for the same reason. The 11728.91 cm-11 band, which was previously introduced as a result of the carbonyl functional group, is not present in the modified substance. This is because oxygen was replaced during chlorination process and opened the way for ethylene diamine to be strengthened.

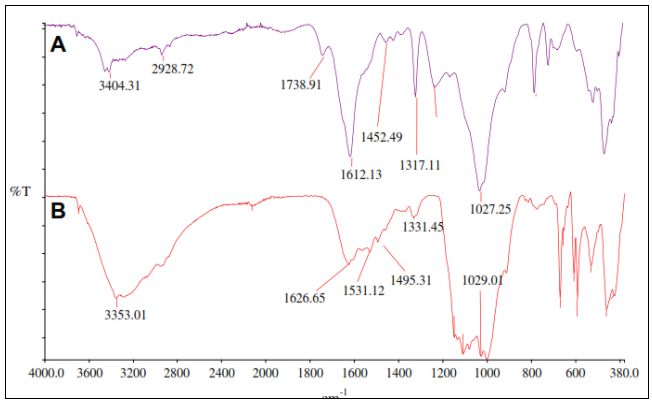

Fig 2: FTIR Spread of Tomato Pulp: (A) Uncorrected and (B) Modified with Ethylenediamine

3.2 NMR results

The results of 13C NMR for tomato scavenger absorption are reported in Fig. 3, in which (A) is not corrected for tomato peel and (B) tomato pumice is modified.

The 13C NMR spectrum shown in Fig. 3 shows the probability of having a similar ring structure with the cellulose in the adsorbent. The peak at δ 178.6 is attributed to the -CO group, which can be related to carboxylate ions.

A small courtyard at δ 130 can be derived from a C = C [10]. The signal between carbon and δ20.0 and δ30.0 in groups Methyl was The adsorbent is likely to contain polysaccharide with repetitive units along its body that contains sulfur and nitrogen in its structure. It has been assumed that the presence of nitrogen and sulfur is a kind of bond between the carbohydrate sector and the peptide of the molecules in its glycosidic bonds. This suggests that tomato pomace may be a sulfate polysaccharide that is usually extracted from tomato pumice, as shown in Fig. 4 A and B of the tomato pulp structure (A) polysaccharide sulfate and (B) glycosaminoglycan given. The results are consistent with Zang *et al*. (2001), which measured the cell wall specification of the yeast by 13C NMR. They reported that signals between δ74.0 and δ105.0 are related to carbohydrates, while paraffinic carbon signals between δ0 and δ45.0 are expected to be olfic carbons between δ125 and δ130. The carboxylic carbon signal is expected to be at δ178.65, which is related to the initial composition of the tomato scum (Alleghe). The observed band at δ178.65 was removed after chlorination, indicating that it was derived from a carbonyl group (-CO) replaced by a chlorine atom. After correction, a new strong signal was observed at δ36 and ø42.0, which was related to the nitrogen carrying carbon carbon atom derived from N-CH2 groups (Torigoe *et al*., 1988). This indicates that ethylenediamine has been successfully absorbed into the absorbent. Comparison of the two spectra shows that different carbonic environments found in the raw material are also found in the modified adsorbent. However, low-power signals that were observed in the modified material were subjected to carbon-induced impacts on solidified groups due to subsidence. A similar phenomenon related to nitrogen bound to carbon atoms was also reported by Schluter (1988), who investigated the preparation of poly (1, 1 and 1) proline preparations with lithium organic markers and subsequent strengths.

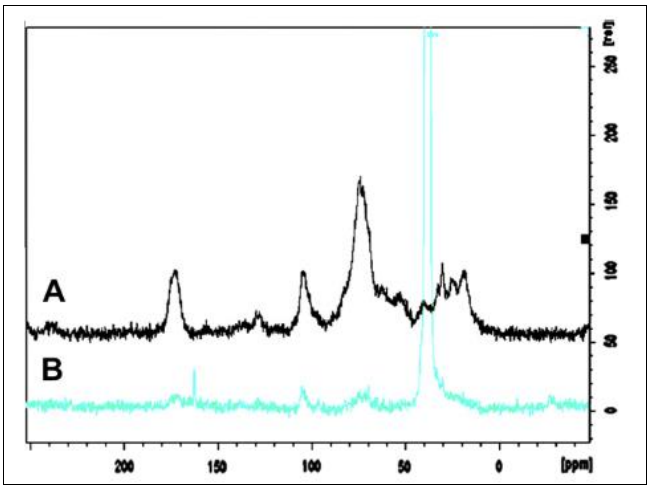

Fig 3: The 13C NMR spectrum is united: Tomato Pumice (A) uncalled and (B) Modified

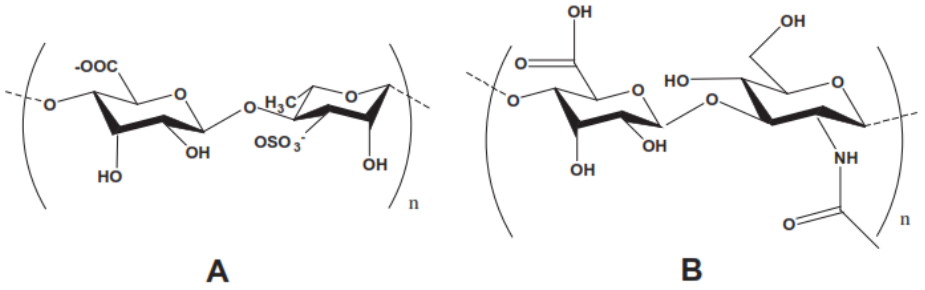

Fig 4: The structure of polysaccharide sulfate (A) and glycosaminoglycan (B) tomato pomace

3.3 Thermal stability

Approximately 10 mg of the sample was heated at -20 ˚C using TGA under nitrogen. Both the modified and unformed tomato pellets are presented in Fig. 4.4. Dementia shows a percentage change in mass (mΔ%) as a function of the sample temperature.

The results show that both modified and unformed tomatoes were lost in weight, but with different rates of destruction. The unpolished absorbent loss rate was very high, so that 50% of the weight disappeared before the temperature reaches 750˚C. At the same temperature range, only 10% of the modified substance is wasted. This study showed that even when increased to 1000˚C, less than 20% of the modified adsorbent was destroyed, suggesting that correction had a significant effect on the thermal stability of tomato scum.

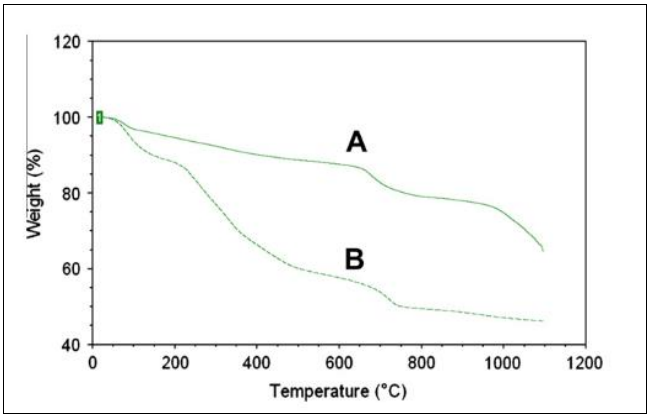

Fig 5: Tomato Pumice Terminology (A) Modified and (B) Unmodified

3.4 Determination of Organic Compound (DOC)

The organic matter content of the DOC was determined by ICP-OES (carbon-based) method with standard carbon-sulfate solution. The analysis was carried out at 247.85 cm-1. A linear plot (y = 485.9x + 283.8) was obtained at a concentration range of 1-100 mg-1 with a slope of 485.9 and a correlation coefficient (R2) of ≥0.999. The content of the DOC was measured between 1.05 ± 1.05 mg mg-1 mg and 9.55 mg-10.03 ± 9.85 mg for unpacked tomato pulp. This indicates that the modification has a significant effect on the reduction of organic matter extraction from the adsorbent into the treated water. Our findings are consistent with the observations made by other researchers that reported DOC values for corrected adsorbent and for purification of metals, mg l-1 19.0-3.8.

3.5 Elemental analysis

The results of elemental analysis indicate that tomato droplets with a composition of 19.86%, 3.09% and 4.14%, respectively, were C, H and N respectively. After correction, the composition of percentage C, H and N was changed to 14.42%, 4.68% and 9.90%. This shows that nitrogen is chemically bonded to the modified tomato pomace structure.

3.6 Effect of pH on absorption

The absorber contains nitrogen atoms (with a single electron pair) along with other functional groups, all of which may be affected by pH. At low pH, the adsorbent has a positive charge because the pH is lower than the isoelectric point or the zero charge point (PZC), in other words pH <PZC. In such a low range of pH, poor absorption is due to the load on the adsorbent. At high pH (pHZP), the adsorbent has a negative charge, which results in high absorption. This is due to the fact that when the metal is present in the solution, it has a positive charge and is absorbed into the adsorbent surface at which the pH (pH> PZC) has a negative charge, which helps to absorb. At pH> 6, metal hydrolysis occurs due to the formation of metal hydroxyl ions, which leads to deposition. The chemical properties of each metal itself alone determine the pH of the maximum absorption. The results of adsorption experiments in different pH values are presented in Fig. 6.

Uncorrected adsorbent had maximum absorption for cadmium at pH 5.2, while the modified adsorbent showed pH 6.3 at its maximum absorbance value. This result is consistent with the results of Singh *et al*. (2006), in which they investigated the adsorption of cadmium using phosphate clay. They observed maximum adsorption at pH 5.4. In this study, the pH value for maximum lead absorption with both unshaped adsorbent and modified adsorbant was 4.4 and 5, respectively. Copper, unlike two other metals, showed a maximum absorption of pH 5.6 at pH 5.6 for modified and unpolished adsorbents. This may be due to the smaller size of copper ions, which gives it a high polar power over adsorbent electrons.

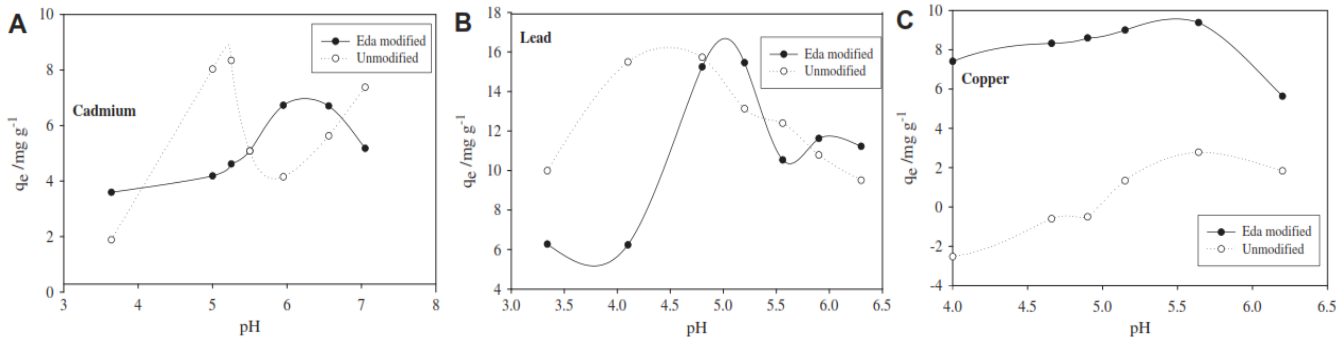

Fig 6: The effect of pH on the adsorption of (c) a) cadmium, (B) lead and (C) copper on the tomato crust modified with ethylamine (in all tests, the amount of adsorbent 0.04 g, the stirring time of 10 minutes and the room temperature)

3.7 Impact of call time

The absorption rate of metal ions is related to the absorption efficiency and the activity of the metal, and thus the novel determines the absorbent residence at a solid-soluble solid state. The adsorption time profile was studied by performing discontinuous adsorption experiments to determine the dependence of the adsorption time of the metal on the time for the modified and unpolished adsorbent. The results of the dependence of time absorption on the graph are presented.

It was observed that the total adsorption rate was rapid until absorption of 90% in 10 minutes, and then the adsorption was carried out at steady state (Fig. 7). The initial rate of absorption in the first 10 minutes can be due to physical absorption or ion exchange at the cell surface, and the subsequent slower phase may be due to other mechanisms such as complex formation, microinjection, or saturation of binding sites. The experimental data obtained for the adsorption of metallic analytes showed that the contact time of 10 minutes was sufficient to achieve maximum absorption, because over time, no further change in concentration was observed. However, in this study, to achieve sufficient time, the equilibrium was set at 30 minutes. As shown in Fig. 7 B, it was observed that the adsorption of cadmium with a modified adsorbent was very low. A decrease in the cadmium uptake was observed, indicating that the responsible groups for binding to cadmium were negatively affected by the correction. An example of the affected functional groups is the carbonyl group, which appeared as peaked in 1738.91 cm-1, as shown in Fig. 7 A and B. This suggests that the carbonyl group has a significant effect on the cadmium bond to the adsorbent. This explains why removing the carbonyl group during chlorination has reduced the ability to absorb adsorbent to cadmium. Tomato scavenging capacity for copper and lead has improved in all directions with reformulation with ethylenediamine.

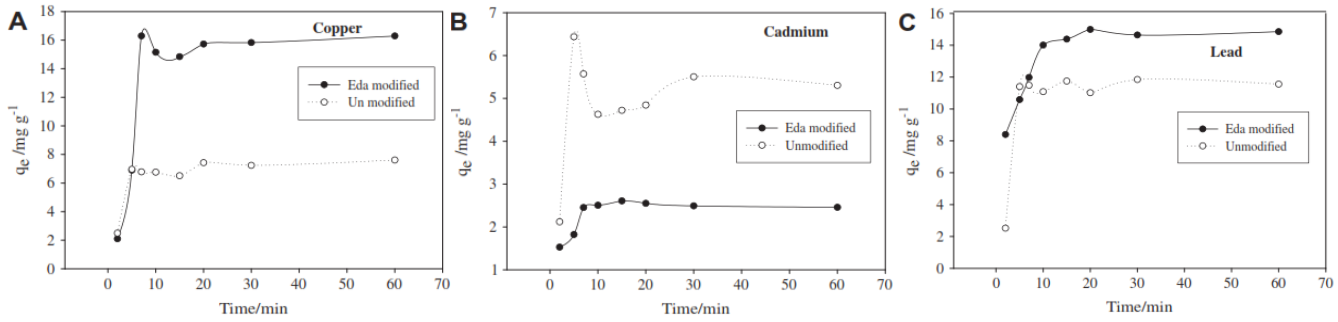

Fig 7: The effect of contact time on the absorption of metal ions on tomato pulp for (a) copper, (b) cadmium, (c) lead

3.8 Kinetic studies

Studies on the absorption rate of metal were studied using Lagrange's first degree kinetics and second order kinetic kinetics. It provides a conceptual representation of the number of molecules involved in each stage of absorption.

The laboratory data was also fitted with the kinetics of the Lagrangian and the kinetics of the octagon. This was done to investigate the molecularity of the absorption mechanism and its speed controlling steps. The kinetic models in Laghouel Lagrange and, respectively, the kinetics of Otdom Ho and colleagues are given in equations 1 and 2, respectively.

$$\ln(C_0 - C_t) = Kt + A \quad (1)$$

$$\frac{1}{q_e} = \mathrm{Kt} + \mathrm{A} \quad (2)$$

Where C_0 is the absorbance per absorbing unit in equilibrium, K is the constant absorption rate, A is the width of the source and C_t is the concentration at time t.

Experimental data for Sarbaba models was obtained from kinetic models in Laghagol Lagrange and also with the kinetics of Ottom Ho and colleagues. A summary of the results from the kinetic data for the metals under study is presented in Table 1.

It was observed that the absorption of cadmium and copper has a pseudo-first kinetics, which indicates that only one species was involved in the speed determination step. While pseudo-quintile kinetics showed the best correlation to absorb lead ions.

Table 1: First-order kinetic data of Lagrange and second order kinetics of Hu *et al.*

Degree of reaction	Pseudo second degree (second order false)	First-order first (false first order)		Metal
	R^2	R^2	Absorbent	
Quasi-second degree	0.743	0.337	Modified	Pb
Quasi-second degree	0.550	0.411	Unmodified	
Pseudo second degree	0.730	0.950	Modified	Cu
Pseudo second degree	0.884	0.904	Unmodified	
Pseudo second degree	0.297	0.550	Modified	Cd
Pseudo second degree	0.568	0.849	Unmodified	

3.9 Effect of initial concentration of metal ion to determine absorption capacity

To investigate the adsorption capacity for the adsorbent modified with ethylenediamine and unsweetened adsorbent, 20 ml of a solution of the model with concentrations in the range of between 40 mg.l^{-1} and 200 mg.l^{-1} were transferred into screw bottles and 100 ml volumes containing g 0.04 were adsorbed and then placed on a mechanical shaker for 30 minutes. The filtered mixture and the metal in solution were analyzed by ICP-OES. The results (Fig. 8) were plotted for mg of absorbed metal per gram of adsorbent (q_e) based on the initial concentration of metal, C_0.

A linear pattern of metal adsorption, followed by a higher metal concentration, was observed in the horizontal graph. This may be due to the saturation of the connection sites, which leads to a steady state. This is because concentrations are the driving force of metal ions to occupy absorption sites.

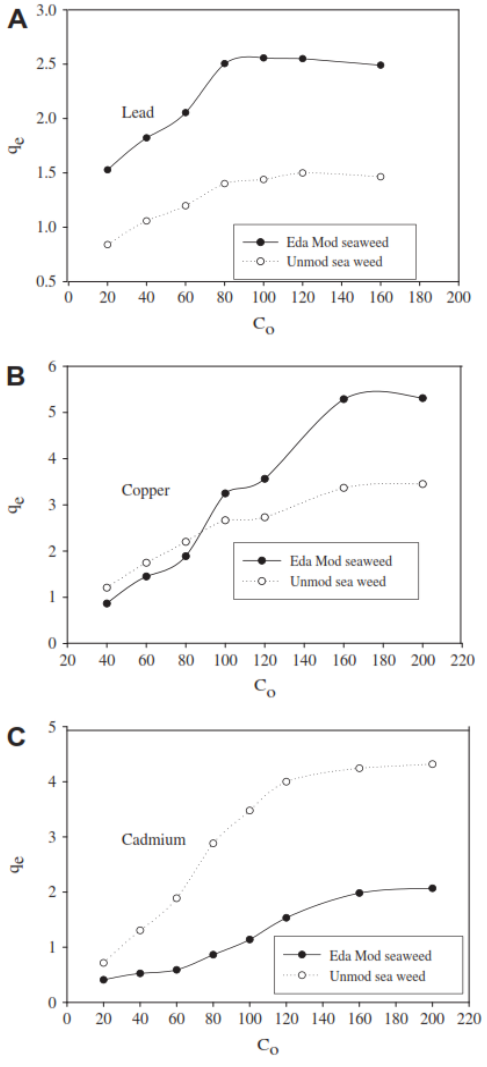

Fig 8: Effect of initial concentration of metal ion on adsorption to determine the adsorption capacity (A) of lead, (B) copper and (C) cadmium

8. Conclusions

This study evaluated the tomato pomace effectively with ethylenediamine. The FT-IR analysis confirmed the presence of functional groups that act as binding sites for metal adsorption. The presence of ethylenediamine carbons in the adsorbent modified by the CP-MAS 13C NMR solid state was confirmed. The content of the adsorbed substance was 5.27 mg. g^{-1}, 2.12 mg. g^{-1} and 2.16 mg. g^{-1} 2.16, respectively, for Cu, Cd and Pb with modified adsorbant, respectively. For unbleached adsorbent, the amounts of mg. g^{-1} were 3.29 mg.g^{-1} 4.57 and 1.05 mg.g^{-1} were reported. However, absorption for cadmium with modified tomato powders showed no improvement as a result of the absence of a carbonyl group that was replaced with ethylenediamine in the modified adsorbent. In addition, a significant improvement in copper and lead ions in water was provided. Copper and cadmium data were well adapted to the Langmuir model (R^2 values for Cu and Cd with the modified substance were 0.866 and 0.964 respectively, and for the unclaimed absorbent 0.999 and 0.950, respectively) indicating the binding mechanism of the laws.

9. References

1. Cong HP, He JJ, Lu Y, Yu SH. Water-Soluble Magnetic-Functionalized Reduced Graphene Oxide Sheets: In situ Synthesis and Magnetic Resonance Imaging Applications. Small, 2010; 6(2):169-173.
2. Ghorbanian B, Khoie SMM. Formation of vanadium carbide with the plasma electrolytic saturation method (PES) and comparison with Thermo Reactive diffusion method (TRD). Acta Metallurgica Slovaca, 2016; 22(2):111-119.
3. Ghorbanian B, Khoie SMM, Rasouli M. Investigation of the Electrolyte Effect on vn Created Via Pes. Acta Metallurgica Slovaca, 2016; 22(4):238-248.
4. Ghorbanian B, Khoie SMM, Rasouli M, Doodran RJ. Investigation of the Electrolyte Effects on Formation of Vanadium Carbide Via Plasma Electrolytic Saturation Method (Pes). Surface Review and Letters, 2016; 23(04):1650021.
5. Hao L, Song H, Zhang L, Wan X, Tang Y, Lv Y. SiO 2/graphene composite for highly selective adsorption of Pb (II) ion. Journal of colloid and interface science. 2012; 369(1):381-387.
6. He F, Fan J, Ma D, Zhang L, Leung C, Chan HL. The attachment of Fe 3 O 4 nanoparticles to graphene oxide by covalent bonding. Carbon, 2010; 48(11):3139-3144.
7. He H, Gao C. Supraparamagnetic, conductive, and processable multifunctional graphene nanosheets coated with high-density Fe3O4 nanoparticles. ACS applied materials & interfaces, 2010; 2(11):3201-3210.
8. Jiang JW, Lan J, Wang JS, Li B. Isotopic effects on the thermal conductivity of graphene nanoribbons: Localization mechanism. Journal of Applied Physics. 2010; 107(5):054314.
9. Kim P, Shi L, Majumdar A, McEuen PL. Thermal transport measurements of individual multiwalled nanotubes. Physical review letters, 2001; 87(21):215502.
10. Lian P, Zhu X, Xiang H, Li Z, Yang W, Wang H. Enhanced cycling performance of Fe 3 O 4–graphene nanocomposite as an anode material for lithium-ion batteries. Electrochimica Acta, 2010; 56(2):834-840.
11. Momeni F, Ghorbanian B, Khoie SMM, Nazari SMM, Rasouli M. Study of Current and Voltage Diagram in The Formed Vanadium Carbide Coatings Via Plasma Electrolytic Saturation Method.
12. Novoselov KS, Jiang D, Schedin F, Booth TJ, Khotkevich VV, Morozov SV, *et al*. Two-dimensional atomic crystals. Proceedings of the National Academy of Sciences of the United States of America, 2005; 102(30):10451-10453.
13. Oostinga J, Heersche H, Liu X, Morpurgo A, Vandersypen L. Gate-tunable band-gap in bilayer graphene devices. *Nature Materials*, 2008; 7:151.
14. Rafiee MA, Rafiee J, Srivastava I, Wang Z, Song H, Yu ZZ, *et al*. Fracture and fatigue in graphene nanocomposites. small, 2010; 6(2):179-183.
15. Singh VK, Patra MK, Manoth M, Gowd GS, Vadera SR, Kumar N. In situ synthesis of graphene oxide and its composites with iron oxide. New carbon materials, 2009; 24(2):147-152.
16. Sundaram RS, Gómez-Navarro C, Balasubramanian K, Burghard M, Kern K. Electrochemical modification of graphene. Advanced Materials, 2008; 20(16):3050-3053.